

Bone spicule pigment formation in retinitis pigmentosa: insights from a mouse model

Gesine B. Jaissle · Christian Albrecht May · Serge A. van de Pavert ·
Andreas Wenzel · Ellen Claes-May · Andreas Gießl · Peter Szurman · Uwe Wolfrum ·
Jan Wijnholds · M. D. Fisher · P. Humphries · M. W. Seeliger

Received: 12 August 2009 / Revised: 31 October 2009 / Accepted: 9 November 2009
© Springer-Verlag 2009

Abstract

Background Bone spicule pigments (BSP) are a hallmark of retinitis pigmentosa (RP). In this study, we examined the process of BSP formation in the rhodopsin knockout (*rho*^{-/-}) mouse, a murine model for human RP.

Methods In *rho*^{-/-} mice from 2 to 16 months of age, representing the range from early to late stages of degeneration, retinal sections and whole mounts were examined morphologically by light and electron microscopy. The results were compared to scanning laser ophthalmoscopy of BSP degeneration in human RP.

Results After the loss of all photoreceptor cells in *rho*^{-/-} mice, the outer retina successively degenerated, leading to approximation and finally a direct contact of inner retinal vessels and the retinal pigment epithelium (RPE). We could show that it was the event of proximity of retinal vessel and RPE that triggered migration of RPE cells along the contacting vessels towards the inner retina. Ultrastructurally, these mislocalized RPE cells partially sealed the vessels by tight junction linkage and deposited extracellular matrix perivascularly. Also, the vascular endothelium developed fenestrations similar to the RPE-choroid interface. In whole mounts,

Supported by DFG grants Se837/1-1, 1-2, 4-1,6-1, Wo 548/6-2, and BMBF grant 0314106.

The authors have full control of all primary data and they agree to allow Graefe's Archive for Clinical and Experimental Ophthalmology to review their data upon request.

Gesine B. Jaissle and Christian Albrecht May contributed equally to this work

M. D. Fisher · M. W. Seeliger
Ocular Neurodegeneration Research Group,
Institute for Ophthalmic Research,
Tuebingen, Germany

G. B. Jaissle (✉) · P. Szurman
University Eye Hospital Tuebingen, Centre for Ophthalmology,
Schleichstr. 12,
72076 Tuebingen, Germany
e-mail: gesine.jaissle@googlemail.com

C. A. May
Department of Anatomy, TU Dresden,
Dresden, Germany

S. A. van de Pavert · J. Wijnholds
Neuromedical Genetics, Netherlands Inst. for Neuroscience,
Amsterdam, The Netherlands

A. Wenzel
Laboratory of Retinal Cell Biology, University Hospital Zürich,
Zürich, Switzerland

E. Claes-May
Max Planck Institute for Brain Research,
Frankfurt/Main, Germany

A. Gießl · U. Wolfrum
Institute for Zoology, University Mainz,
Mainz, Germany

P. Humphries
Ocular Genetics Unit, Trinity College, Smurfit Institute,
Dublin, Ireland

Present Address:

A. Gießl
Dept. of Biology and Animal Physiology,
University of Erlangen-Nuernberg,
Erlangen, Germany

the pigmented cell clusters outlining retinal capillaries correlated well with BSPs in human RP. The structure of the inner retina remained well preserved, even in late stages. **Conclusions** The *Rho*^{-/-} mouse is the first animal model that depicts all major pathological changes, even in the late stages of RP. Using the *rho*^{-/-} mouse model we were able to analyze the complete dynamic process of BSP formation. Therefore we conclude that: (1) In *rho*^{-/-} retinas, BSPs only form in areas devoid of photoreceptors; (2) Direct contact between inner retinal vessels and RPE appears to be a major trigger for migration of RPE cells; (3) The distribution of the RPE cells in BSPs reflects the vascular network at the time of formation. The similarity of the disease process between mouse and human and the possibility to study all consecutive steps of the course of the disease makes the *rho*^{-/-} mouse valuable for further insights in the dynamics of BSP formation in human RP.

Keywords Bone spicule pigment formation · Rhodopsin knockout · Mouse model · Retinitis pigmentosa · Outer retina · Retinal degeneration

Introduction

Retinitis pigmentosa (RP) refers to a group of clinically similar but genetically heterogeneous hereditary rod-cone degenerative disorders. The incidence of RP is estimated to be 1 in 4,000, which makes it one of the most common causes of severe visual impairment in humans [1, 2]. RP gives rise to a primary loss of photoreceptors followed by degeneration of the outer layers of the retina, whereas the inner retina is widely preserved until late in the course of the disease [3, 4]. A hallmark of typical RP is the presence of intraretinal melanin deposits that can be identified as bone spicule pigments (BSP) on ophthalmoscopy [1–3]. Despite many details of such pigmentation that have been described in the past [3, 5–12] there has been no comprehensive study on the nature of BSPs and especially the conditions for their development. One reason may be that the access to donor eyes is limited, and histomorphological studies on human patients concerned small numbers of advanced cases of RP [5, 7–9, 11], which restrict characterization of the dynamic process of the disease. Hence, we based our work on a murine homologue of an autosomal-recessive form of human RP, the rhodopsin knockout (*rho*^{-/-}) mouse in which the rhodopsin gene is disrupted [13]. Comparable to human RP, the homozygous genetic defect causes a complete lack of rod outer segments and rod function leading to a quick loss of rod photoreceptors [13–15]. Consecutively, progressive cone degeneration develops, being complete at approximately 3 months of age [13–16]. Previously, we could show that young *rho*^{-/-} mice can serve as a model for pure cone function

in a limited time interval when cone function is already sufficiently developed but cone degeneration is not yet substantial [15]. Former studies have been restricted to the first 3–4 months of age, but long-term investigations on advanced degenerative stages specific for RP have not yet been reported [13–18]. Considering the similarities of the *rho*^{-/-} mice at early stages with RP patients, one might assume that investigations on the further degeneration process could also provide a better understanding of late cellular interactions following photoreceptor death in the human disease. Although vast information is available about detailed histological changes in later, more severe forms of RP, little is known about the dynamic disease process. Neovascularization of the RPE has been described after loss of photoreceptor cells in transgenic mice [19], but the underlying mechanisms that cause migration of RPE cells to perivascular sites in the inner retina finally leading to the formation of BSP are still unknown [3, 10]. Furthermore, it is unclear why BSP is typically observed in areas that lack photoreceptors [3].

Therefore, we have carefully examined if there is a comparable formation of BSP in the ageing *rho*^{-/-} retina as observed in human RP. Existence of BSPs in the *rho*^{-/-} mouse would provide a valuable model to investigate the dynamic process of BSP formation and to transfer these findings to the human disease.

Materials and methods

Animals

The study was conducted on *rho*^{-/-} mice that carried a targeted disruption of exon 2 of the rhodopsin gene leading to a complete lack of rhodopsin [13]. To investigate the full degenerative process of the retina following loss of the photoreceptors, mice of different ages ranging from 2 to 16 months were used. Age-matched C57Bl/6 mice served as controls, as the *rho*^{-/-} mice were on a C57Bl/6 background. All experiments in this study were performed in accordance with the institutional animal guidelines and according to the ARVO Statement for Use of Animals in Ophthalmic and Vision Research and the local animal care rules.

Histology

Light and electron microscopy

For electron microscopy, four *rho*^{-/-} animals (EM: 3, 6, 12, and 14 months) and eight age-matched C57Bl/6 mice were perfused with 4% paraformaldehyde (PFA), enucleated, and postfixed in a solution containing glutaraldehyde (2.5%), PFA (2.5%), and picric acid (0.05%) in cacodylate buffer (pH 7.3).

After rinsing in cacodylate buffer and dissection, small specimens were immersed in 1% OsO₄, dehydrated in ascending series of alcohols, and embedded in Epon or Araltit according to standard methods. Semithin sections were stained with toluidine blue, ultrathin sections were stained with uranyl acetate and lead citrate and viewed in an electron microscope (EM 902, Zeiss, Oberkochen, Germany or Tecnai 12 BioTwin transmission electron microscope, FEI, The Netherlands).

For Technovit sections, eyes were enucleated, fixed, and 3- μ m sections (Technovit 7100, Kultzer, Wehrheim, Germany) were counterstained with toluidine blue.

For Nomarski micrographs, *rho*^{-/-} mice (2 and 8 months), and an adult C57Bl/6 mouse (2 months) were deeply anesthetized with halothane, decapitated, and the eyes removed. The posterior eyecup was immersion-fixed in 4% paraformaldehyde in 0.1 M phosphate buffer for 15 min. The retinas were dissected from the eyecup, cryoprotected in graded sucrose solutions (10–30%), and sectioned vertically at 14 μ m on a freezing microtome. Nomarski micrographs were stained with anti-Mouse Serum Albumin AB (Nordic Immunological Laboratories, The Netherlands) as primary antibody for blood serum albumin to identify retinal vascular lumina. Goat anti-rabbit CY3 (Jackson ImmunoResearch) was used as secondary antibody.

Retinal whole mounts

PFA-perfused eyes of six *rho*^{-/-} animals (6, 12, and 16 months) and of 12 age-matched C57Bl/6 mice were used to perform retinal and choroido-scleral whole mounts. After rinsing in PBS, the whole mounts were incubated in a solution containing 0.1 mg/ml nitroblue tetrazolium, 1 mg/ml NADPH, and 0.3% Triton X-100 in 0.01 M PBS at 37°. The reaction was stopped in cold PBS after 1–2 h and the whole mounts were mounted on glass slides with glycerin jelly.

Indirect immunofluorescence

Bassoon-calretinin double staining

After preparing vertical sections of the mouse retina, slices were washed in PBS and secondary antibodies (mouse monoclonal antibody against the cytomatrix protein bassoon to visualize rod spherules (Stressgen Biotechnologies, Canada; 1:5000), and mouse anti-calretinin to stain horizontal, amacrine and ganglion cells (Chemicon International Inc., Temecula, CA; 1:2000) were applied overnight at room temperature. After washing in PBS, secondary antibodies were applied for 1 h. These were conjugated either to Alexa TM 594 (red fluorescence) or Alexa TM 488 (green fluorescence) (Molecular Probes, Eugene, Oregon). Confocal micrographs were taken of an adult C57Bl/6 mouse (2 months) and *rho*^{-/-} mice

(2 and 8 months) using a Zeiss LSM5 Pascal confocal microscope equipped with an argon and helium-neon laser.

CD31-DAPI double staining

Eyes of adult C57Bl/6 mice and a *rho*^{-/-} mouse at 3 months of age were cryofixed in melting isopentane, cryosectioned, and treated as previously described [20, 21]. Retinal cryosections were stained with anti-CD31 (BD Pharmingen, USA) as a molecular marker for the endothelium of blood vessels. Secondary antibodies to rat IgG were purchased as conjugates to Alexa 488 (Molecular Probes). Nuclei of retinal cells were counterstained with 4',6'-diamidino-2-phenylindole (DAPI). Sections were mounted in Mowiol 4.88 (Farbwerke Hoechst, Frankfurt, Germany), containing 2% *N*-propyl gallate. No reactions were observed in control sections. Mounted retinal sections were examined with a Leica DMRP microscope. Images were obtained with a Hamamatsu ORCA ER charge-coupled device camera (Hamamatsu, Germany) and processed with Adobe Photoshop (Adobe Systems, USA).

Optical coherence tomography (OCT) in a human RP patient

The scanning laser ophthalmoscopic (SLO) image and the corresponding OCT scans were obtained with a Heidelberg Engineering Spectralis (Heidelberg Engineering, Dossenheim, Germany) in a patient with advanced RP. This examination followed the tenets of the Declaration of Helsinki.

Results

Loss of the outer retina, preservation of the inner retina

As previously described, the lack of rhodopsin in the *rho*^{-/-} mice led to characteristic changes in the early course of RP especially a disability to form rod outer segments (OS) and consecutively to an early loss of rod photoreceptor cells. Like in human RP, cones were initially spared but degenerated some 4–6 weeks later, leading to a successive loss of all layers of the outer retina [3, 14, 15]. Figure 1a, b illustrates the situation at 2 months of age. Rod OS were absent, and both the inner segments (IS) and the outer nuclear layer (ONL) were significantly reduced compared to control mice due to rod photoreceptor cell loss. At 8 months of age, the outer retina was practically fully degenerated with a complete loss of OS, IS, and ONL (Fig. 1c). However, remnants of rod spherules in the outer plexiform layer (OPL) were still present (Fig. 1f). Despite the loss of the outer retina, the inner retina remained well preserved, even at late stages: at 2 months of age, immunohistochemical staining identified a regular inner

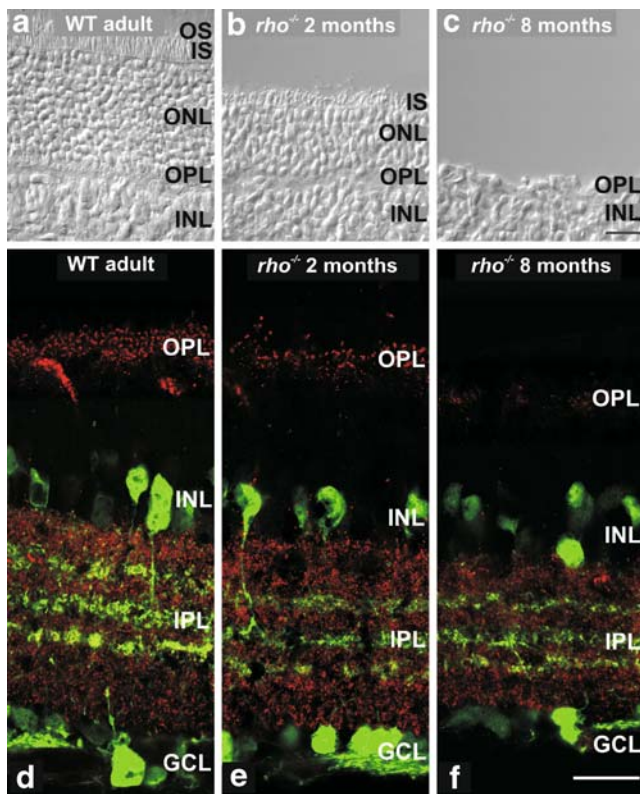


Fig. 1 Stages of retinal degeneration in the $\rho^{-/-}$ mouse. *Top row:* Cryosections (Nomarski differential interference contrast optics) of early and late stages of retinal degeneration in $\rho^{-/-}$ mice. **a** Regular architecture of the outer retina in an adult control wild type (WT) mouse. **b** Early stage of retinal degeneration in a $\rho^{-/-}$ mouse at 2 months of age. Note missing OS layer and changes of the IS layer and ONL due to the rod defect. **c** Late-stage retinal degeneration in a $\rho^{-/-}$ mouse at 8 months of age. The outer retina has practically vanished and only remnants of the OPL are left. *Bottom row:* Immunostainings at corresponding time points demonstrate preservation of the inner retina (rod spherules are visualized using Bassoon, red, and Calretinin staining demonstrates horizontal, amacrine and ganglion cells, green). **d** Normal synaptic layers in the OPL and IPL in an adult control. **e, f** Increased loss of rod spherules in the synapses of the OPL (indicated by Bassoon) in $\rho^{-/-}$ mice at 2 and 8 months of age. The INL and the IPL layering appear to be preserved even at 8 months of age

nuclear layer (INL), inner plexiform layer (IPL), and ganglion cell layer (GCL) very similar to the control mouse (Fig. 1d, e). At 8 months of age, the inner retinal layers were only slightly reduced in height, and the IPL (with the typical stratification pattern), the INL, and the GCL were still well preserved (Fig. 1f).

Initiation of RPE cell migration

The loss of photoreceptors alters retinal integrity in many ways. Most obvious is the reduction in retinal thickness, since the space vacated by the photoreceptors is filled by the inner retinal layers passively moving downwards in the direction of the RPE (approximation). Figure 2a, b

illustrates this approximation in a $\rho^{-/-}$ animal with only 1–2 rows of (cone) photoreceptors left in comparison to a normal control. Of particular importance is the position of retinal vessels relative to the RPE layer (arrows in Fig. 2a–b). In the normal retina, retinal vessels are separated from the RPE by the relatively thick photoreceptor layer (PRL), and no vessels are located in either the PRL or the ONL or the RPE (Fig. 2a). However, following the strong reduction and, finally, the loss of the PRL in the $\rho^{-/-}$ mice, the retinal vessels of the inner retina seem to approximate and get in close vicinity to the RPE layer (Fig. 2b).

With complete loss of the outer retina at around 8–10 months of age, these retinal vessels finally come into direct contact with the RPE. Once the contact is made, this event initiates a migratory behavior of the local RPE cells. Figure 2c illustrates an early stage of this process: The RPE cells touching retinal vessels start to migrate towards and finally surround them (arrow in inset of Fig. 2c), so that the vessels appear to be covered with the RPE cells (arrowheads in Fig. 2c).

Nature of RPE cell migration

In all specimens examined, RPE cell migration and epithelial cuff formation around retinal vessels is closely related to the presence of a direct vascular contact (Fig. 3). This suggests that the close contact between RPE and an approximating vessel (of the inner retina) is a stimulus for the RPE cells to detach from Bruch's membrane and to migrate along the adjacent retinal vessel to perivascular sites in the inner retina (Fig. 3a–c). Here the RPE cells strictly align with their basal side towards the vessels. Interestingly, this newly formed interface is similar to the RPE/choriocapillaris interface and includes intercellular seals with tight junctions, deposited extracellular matrix (ECM) between the relocated RPE cells, and the vascular endothelial cells (Fig. 3d–e), and endothelial fenestration (arrow in Fig. 3e).

Bone spicule pigment formation

At rather progressed stages, BSP formation is widespread across the retina. In flat mount preparations at 16 months of age, both the topographical distribution as well as the considerable extent of vessel cuffing is visible (Fig. 4a–d). These specimens are obtained by removing the neuroretina from the eyecup, usually leaving RPE and choroid in place. However, in late-stage RP, the RPE cells that had migrated into the neuroretina become removed during the preparation process. Typically, the nuclei of the migrated RPE cells are translucent, whereas the cell body is dark due to melanin, and they form three-dimensional pigmented cell clusters around retinal vessels (Fig. 4a). These pigmented cell

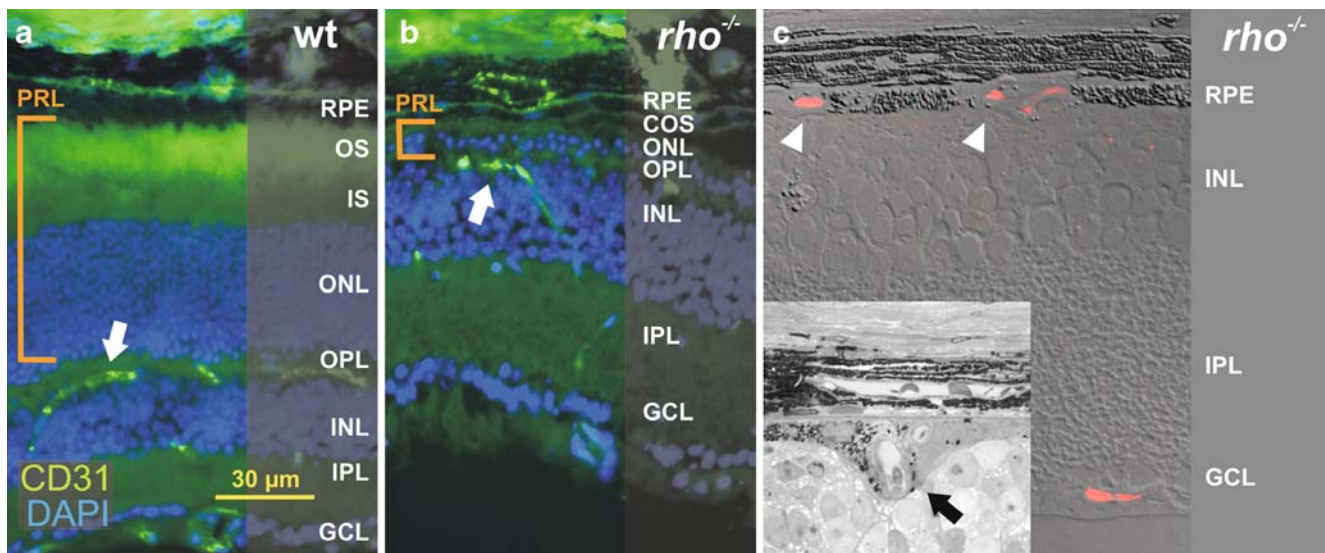


Fig. 2 Process of vascularization of the RPE, a prerequisite for bone spicule pigment formation. Vascularization of the RPE is the result of a passive, degenerative phase (successive, selective loss of photoreceptors as in **b**), which is followed by an active, proliferative phase (outgrowth of RPE cells upon contact with retinal capillaries as in **c**) leading to BSP formation. **a, b** Immunofluorescence analysis of retinal cryosections by anti-CD31 (green), a molecular marker for endothelia (blood vessels), indicating the position of retinal blood vessels (arrows) relative to retinal layers (**a**, adult control mouse, and **b**, $\rho^{-/-}$ mouse with advanced degeneration of the outer retina). Nuclei

of retinal cells counterstained with DAPI (blue). For comparison, the thickness of the photoreceptor layer (PRL) is marked with a bracket. Note the close vicinity of the retinal capillaries in the OPL (arrow) to the RPE in **b**. **c** Normarski contrast image merged with serum albumin staining of retinal vascular lumina (red) in a $\rho^{-/-}$ mouse retina with advanced degeneration. Note that the retinal capillaries usually running in the OPL (indicated by arrowheads) are included in the RPE. *Insert*: Light micrograph cross section of a retinal vessel in (normally never occurring) direct contact with the RPE. RPE cells are displaced at these locations and actively surround the capillary (arrow)

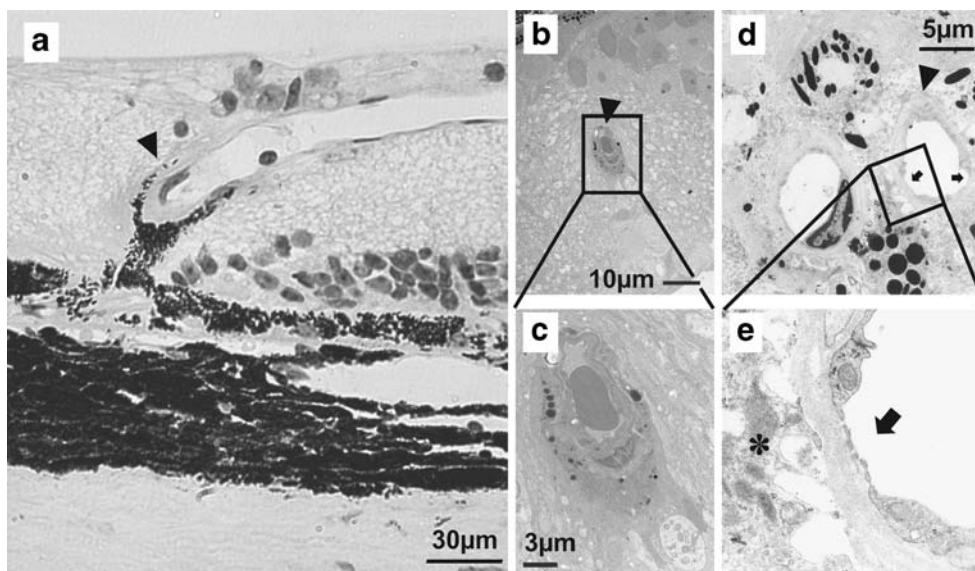


Fig. 3 RPE cell migration along retinal vessels in $\rho^{-/-}$ mice at late stages. Upon initiation of the active phase, RPE cells migrate upwards along the retinal capillaries. The newly formed RPE-vessel interface resembles that between RPE and choriocapillaris, including tight junction seals, ECM, and endothelial fenestrations. **a** Light micrograph of a retinal vessel in the inner retina surrounded by apparently upward migrating RPE cells. **b, c** Transmission electron micrographs

of cross sections of a retinal vessel (indicated by an arrowhead) in the inner retina that are sheathed by presumed RPE cells. Note pigment granules. **d** Transmission electron micrographs of a cross section of a retinal capillary (arrowhead), illustrating fenestrations of the vessel (arrows). **e** (detail of **d**) arrow indicates the endothelial fenestrations; ECM is indicated by an asterisk

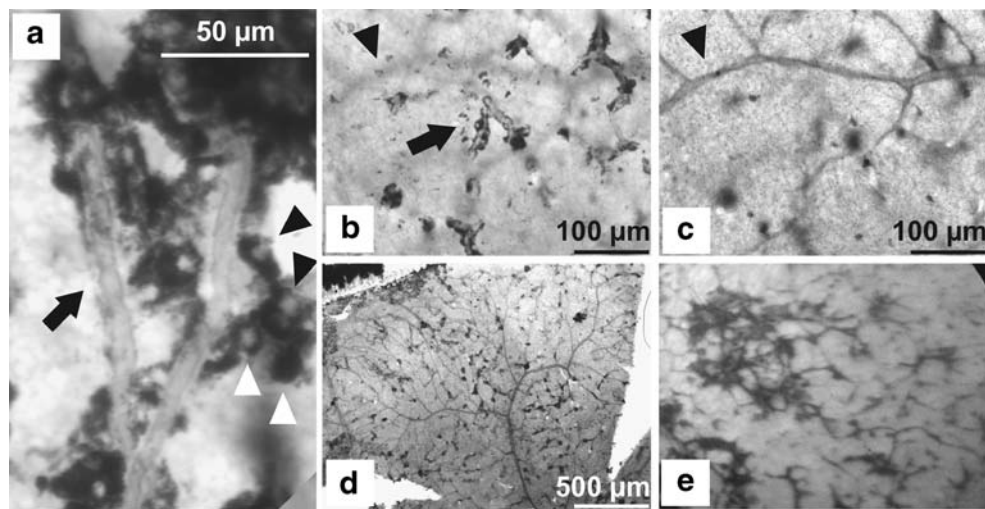


Fig. 4 Distribution of bone spicule pigment across the retina. BSPs approximately delineate the retinal capillary network at the time they formed. **a** RPE cells (*arrowheads*) located along retinal capillaries (*arrow*) in a flat-mount preparation (NADPH diaphorase staining). Note the centrally brighter area due to the melanin-free nucleus. **b** Detail of the inner retina (INL) at lower magnification (same layer as A). The *arrow* points to a retinal capillary surrounded by pigmented

cells. The *arrowhead* indicates the same location in **b** and **c**. **c** Same detail as **b** but focused on the IPL, allowing visualizing retinal surface vessels. **d**, **e** Low magnification view of an entire retinal quadrant (**d**) in comparison to a fundus image of a human patient with RP (**e**). The clumps and elongated formations of pigmented cells along the retinal vessels in mice resemble very well BSPs in humans

formations around retinal vessels can be found in practically all retinal areas in *rho*^{-/-} mice (Fig. 4b, d). In late stages, these pigmented cell clusters cover most of the capillaries, but stay short of the large surface vessels (Fig. 4c). This pattern (Fig. 4a–d) resembles well the characteristic BSP formations in advanced human RP (Fig. 4e).

Ocular coherence tomography (OCT) in a human RP patient

The SLO image in Fig. 5 depicts a paramacular area with BSPs in a human RP patient. Notably, the region where BSPs are found also shows a remarkable atrophy of retina and RPE. The three sections (Fig. 5a–c) show BSP at

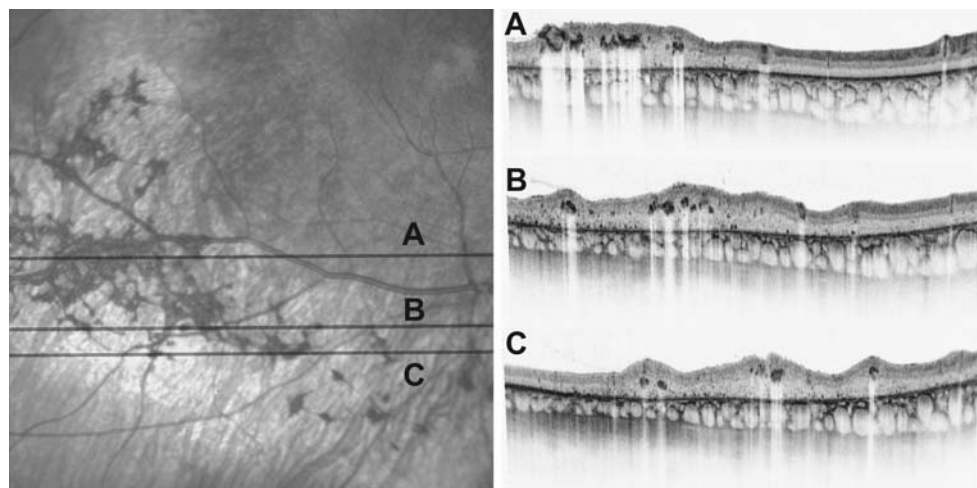


Fig. 5 OCT of a human RP patient. SLO image (*left*) of the paramacular area of a patient with RP. The fovea is located in the *upper right corner*. Note the atrophy of retina and RPE in the region where BSPs are abundant. The three sections (*A–C*) illustrate the retinal location of BSP. Most of the large, confluent pigment clumps are located in or just below the GCL. Their melanin content strongly

absorbs light and thus causes a “shadow” effect. Notably, the thickness of the retina is increased where extensive pigmentation is present. In addition, several smaller pigment clumps are located between the RPE and the GCL, which most probably resemble the cuffs around vessels of different size and height

different layers and in different sizes. Most obvious are the confluent, large pigment clumps mainly located below the GCL, which absorb most of the light and thus cause a “shadow” below. Where these are present, the thickness of the retina is increased. However, between the RPE layer and the GCL, several smaller pigment arrangements are visible, which most probably resemble the cuffs around vessels of different size.

Discussion

In this work, we have shown the *rho*^{-/-} mouse to be the first animal model available featuring morphologically the course of degeneration of RP in all fundamental phases including the late stages. Based on this model we could investigate the process of formation of BSP and demonstrated that the direct contact of RPE and retinal vessels appears to be a key factor.

In a number of histological studies on human donor eyes, BSPs were found only in areas devoid of photoreceptors, and were formed by RPE cells migrating along retinal vessels [3, 8–12]. However, the trigger for detachment of RPE cells from Bruch's membrane and successive migration has still remained unclear. Our results demonstrate that RPE migration is closely related to the selective, complete loss of rod and cone photoreceptor cells, thereby allowing inner retinal vessels from the OPL to approximate and make contact with the apical side of the RPE. Moreover, we could demonstrate for the first time that this direct contact seems to cause RPE cells to detach from Bruch's membrane and to migrate along the contacting vessels towards the inner retina. Our murine whole-mount data illustrate the arrangement of pigmented cell clusters outlining retinal capillaries that correlate well with BSPs in humans [3, 8–12]. Moreover, using OCT investigation in an RP patient we could demonstrate perivascular pigmentation *in vivo*, thereby proving that BSPs are located at different retinal layers ranging from the RPE to the GCL comparable to our findings in the mouse model.

It has been speculated as to why RPE cells are attracted by retinal vessels. The affinity of RPE cells to vascular basal lamina or ECM around retinal blood vessels might play a role [3, 8, 10]. Alternatively, the release of cytokines from vascular endothelium has been suggested as a factor that might trigger RPE migration [3, 10]. Potentially, actual blood flow in the vessels accounting for higher oxygen levels might also be a factor for the attraction of RPE cells. Therefore, we hypothesize that BSPs grow in the presence of vascular flow. Interestingly, our OCT investigation in a RP patient showed that the thickness of the retina was less reduced around areas of heavy pigmentation. Therefore, it might be assumed that the relatively better vascular supply

accounted for the preservation of the inner retina at these sites. Also, preservation of the retinal thickness might be due to a firm RPE cell cast of the vascular system at the time before pronounced degeneration of the inner retina was present. This might have prevented thinning of the retina later in the course of the disease. However, other presently unknown mechanisms might also play a role.

Since vascular changes have been found to be secondary to photoreceptor damage [2, 22], it has been proposed that retinal arteriolar constriction, one of the key findings in RP, is the result of (1) increased intravascular oxygen tension due to decreased oxygen consumption by the degenerating outer retinal layers and/or (2) closer proximity of the retinal vascular network to the choroidal circulation as a result of retinal thinning [2]. In other words, retinal blood flow may be substantially reduced *before* the final row of photoreceptors is lost. Given that vascular flow is a major stimulus for RPE migration, the stimulus strength might be different at the time migration starts. Hence, this is a possible explanation for variables in the amount and distribution of pigmentation among different RP genotypes assuming differences in the mechanism and speed of the degeneration.

Based on our data, one might speculate that RPE migration and BSP formation is an attempt to form a leakage-proof blood/retina barrier similar to the RPE/choriocapillaris interface. As we have shown ultrastructurally, the migrating RPE cells behaved similar to those at the RPE-choroidal interface: they sealed the vessels by tight junction linkage, deposited perivascular ECM, and (presumably by polarized VEGF secretion [23]) induced fenestrations in the vascular endothelium of cuffed vessels comparable to those in the choriocapillaris. Also, the translocated cells were remarkably polarized with their basal side towards the vessel characteristic of RPE cells *in situ*. Such behavior has also been described in RP patients [8, 10] and in other animal models [22, 24]. Li and colleagues found vascular endothelial cells separated from the translocated RPE cells by a layer of extracellular matrix similar in organization to Bruch's membrane [10]. Therefore, preexistence of ECM that might serve as a leading structure for RPE migration cannot be ruled out [8, 10]. As we have shown, direct contact between vessels and RPE appears to be essential for BSP formation. However, a transgenic animal model expressing VEGF in rod photoreceptors demonstrated that absence of photoreceptors is not necessarily required [24, 25]. The model showed a pathological ingrowth of retinal vessels originating from the deep capillary bed into the subretinal space that caused contact with the RPE even in the presence of regular rod and cone photoreceptors. Based on our findings one can deduce that the pathological direct contact of retinal vessels and RPE layer stimulated the RPE cells to react in the same characteristic way: They migrated to surround the aberrant

vessels, deposited ECM, and reestablished the blood–retina barrier by forming tight junctions thereby reducing leakage from vascular endothelial fenestrations. Our dynamic mouse model allowed for the first time to reason that it is the anatomical close proximity of retinal vessels and RPE that seems to be the key factor for RPE migration and formation of BSP. This disease sequence seems to be a general process in retinal degeneration, also in RP patients.

In conclusion, we found that BSPs only form in areas with direct contact of inner retinal vessels and RPE that is usually caused by a loss of photoreceptors and the outer retinal layers. This contact seems to be a major trigger for the migration of RPE cells along the contacting retinal vessels. The distribution of the BSP seems to reflect the status of the retinal vascular network at the time of formation. The substantial similarity of the course of the disease between mouse and human and the possibility to access the dynamic disease process makes the *rho*^{-/-} mouse a valuable model to obtain further insights in the dynamics of BSP formation.

Acknowledgements The authors thank Dr. Dominik Fischer for the SLO investigation.

Financial interest None.

References

- Hartong DT, Berson EL, Dryja TP (2006) Retinitis pigmentosa. *Lancet* 368:1795–1809
- Pagon RA (1988) Retinitis pigmentosa. *Surv Ophthalmol* 33:137–177
- Milam AH, Li ZY, Fariss RN (1998) Histopathology of the human retina in retinitis pigmentosa. *Prog Retin Eye Res* 17:175–205
- Santos A, Humayun MS, de Juan E, Greenburg RJ, Marsh MJ, Klock IB, Milam AH (1997) Preservation of the inner retina in retinitis pigmentosa. A morphometric analysis. *Arch Ophthalmol* 115:511–515
- Lahav M, Craft J, Albert DM, Ishii Y (1982) Advanced pigmentary retinal degeneration. An ultrastructural study. *Retina* 2:65–75
- Milam AH, Kalina RE, Pagon RA (1983) Clinical-ultrastructural study of a retinal dystrophy. *Invest Ophthalmol Vis Sci* 24:458–469
- Szamer RB, Berson EL (1977) Retinal ultrastructure in advanced retinitis pigmentosa. *Invest Ophthalmol Vis Sci* 16:947–962
- Milam AH, De Castro EB, Smith JE, Tang WX, John SJ, Gorin MB, Stone EM, Aguirre GD, Jacobson SG (2001) Concentric retinitis pigmentosa: clinicopathologic correlations. *Exp Eye Res* 73:493–508
- Li ZY, Jacobson SG, Milam AH (1994) Autosomal dominant retinitis pigmentosa caused by the threonine-17-methionine rhodopsin mutation: retinal histopathology and immunocytochemistry. *Exp Eye Res* 58:397–408
- Li ZY, Possin DE, Milam AH (1995) Histopathology of bone spicule pigmentation in retinitis pigmentosa. *Ophthalmology* 102:805–816
- To K, Adamian M, Dryja TP, Berson EL (2002) Histopathologic study of variation in severity of retinitis pigmentosa due to the dominant rhodopsin mutation Pro23His. *Am J Ophthalmol* 134:290–293
- Flannery JG, Farber DB, Bird AC, Bok D (1989) Degenerative changes in a retina affected with autosomal dominant retinitis pigmentosa. *Invest Ophthalmol Vis Sci* 30:191–211
- Humphries MM, Rancourt D, Farrar GJ, Kenna P, Hazel M, Bush RA, Sieving PA, Sheils DM, McNally N, Creighton P, Erven A, Boros A, Gulya K, Capecchi MR, Humphries P (1997) Retinopathy induced in mice by targeted disruption of the rhodopsin gene. *Nat Genet* 15:216–219
- Toda K, Bush RA, Humphries P, Sieving PA (1999) The electroretinogram of the rhodopsin knockout mouse. *Vis Neurosci* 16:391–398
- Jaissle GB, May CA, Reinhard J, Kohler K, Fauser S, Lütjen-Drecoll E, Zrenner E, Seeliger MW (2001) Evaluation of the rhodopsin knockout mouse as a model of pure cone function. *Invest Ophthalmol Vis Sci* 42:506–513
- Humphries MM, Kiang S, McNally N, Donovan MA, Sieving PA, Bush RA, Machida S, Cotter T, Hobson A, Farrar J, Humphries P, Kenna P (2001) Comparative structural and functional analysis of photoreceptor neurons of Rho^{-/-} mice reveal increased survival on C57BL/6J in comparison to 129 Sv genetic background. *Vis Neurosci* 18:437–443
- Hobson AH, Donovan M, Humphries MM, Tuohy G, McNally N, Carmody R, Cotter T, Farrar GJ, Kenna PF, Humphries P (2000) Apoptotic photoreceptor death in the rhodopsin knockout mouse in the presence and absence of c-fos. *Exp Eye Res* 71:247–254
- Campbell M, Humphries M, Kennan A, Kenna P, Humphries P, Brankin B (2006) Aberrant retinal tight junction and adherens junction protein expression in an animal model of autosomal dominant Retinitis pigmentosa: the Rho^(-/-) mouse. *Exp Eye Res* 83:484–492
- Nishikawa S, LaVail MM (1998) Neovascularization of the RPE: temporal differences in mice with rod photoreceptor gene defects. *Exp Eye Res* 67:509–515
- Wolfgram U (1991) Centrin- and alpha-actinin-like immunoreactivity in the ciliary rootlets of insect sensilla. *Cell Tissue Res* 266:31–38
- Reiners J, Reidel B, El-Amraoui A, Boëda B, Huber I, Petit C, Wolfgram U (2003) Differential distribution of harmonin isoforms and their possible role in Usher 1 protein complexes in mammalian photoreceptor cells. *Invest Ophthalmol Vis Sci* 44:5006–5015
- Penn JS, Li S, Naash MI (2000) Ambient hypoxia reverses retinal vascular attenuation in a transgenic mouse model of autosomal dominant retinitis pigmentosa. *Invest Ophthalmol Vis Sci* 41:4007–4013
- Blaauwgeers HG, Holtkamp GM, Rutten H, Witmer AN, Koolwijk P, Partanen TA, Alitalo K, Kroon ME, Kijlstra A, van Hinsbergh VW, Schlingemann RO (1999) Polarized vascular endothelial growth factor secretion by human retinal pigment epithelium and localization of vascular endothelial growth factor receptors on the inner choriocapillaris. Evidence for a trophic paracrine relation. *Am J Pathol* 155:421–428
- Roque RS, Caldwell RB (1991) Pigment epithelial cell changes precede vascular transformations in the dystrophic rat retina. *Exp Eye Res* 53:787–798
- Ida H, Tobe T, Nambu H, Matsumura M, Uyama M, Campochiaro PA (2003) RPE cells modulate subretinal neovascularization, but do not cause regression in mice with sustained expression of VEGF. *Invest Ophthalmol Vis Sci* 44:5430–5437